Ecotoxicology and Environmental Safety 130 (2016) 155–162

Contents lists available at ScienceDirect

Ecotoxicology and Environmental Safety

journal homepage: www.elsevier.com/locate/ecoenv

Effectiveness and potential of straw- and wood-based biochars for adsorption of imidazolium-type ionic liquids

Kaishun Shi [a], Yuping Qiu [a,b,*], Ben Li [b], Michael K. Stenstrom [b]

[a] State Key Laboratory of Pollution Control and Resource Reuse, College of Environmental Science and Engineering, Tongji University, Shanghai 200092, China
[b] Civil and Environmental Engineering Department, University of California, 5732 Boelter Hall, Los Angeles 90095-1593, USA

ARTICLE INFO

Article history:
Received 29 February 2016
Received in revised form
11 April 2016
Accepted 12 April 2016

Keywords:
Ionic liquids
Adsorption
Removal
Biochars

ABSTRACT

The growing industrial application of imidazolium-type ionic liquids (ITILs) is likely to result in their release to the environment. Water-soluble ITILs are difficult to remove from wastewaters using traditional adsorbents. In this work, we developed different biochars derived from straw and wood (named as SBB and WBB, respectively) to improve the adsorption effectiveness for removal of ITILs from wastewaters. SBB had high O/C element ratio (0.143), while WBB had high ratio of V_{micro}/V_{total} (61.5%) compared with commercial activated carbon (AC). Both of them showed greater adsorption of ITILs than AC with different adsorption mechanisms. FTIR spectra revealed that electrostatic interactions were the dominant driving force in SBB adsorption, while high micropore volume promoted adsorption in WBB. The adsorption of $[C_2mim][BF_4]$ on SBB and WBB was strongly enhanced by trivalent PO_4^{3-} anions, suggesting that PO_4^{3-} anions could be used as promoter to increase the removal efficiency of ITILs from wastewater. Using HCl solution (pH=0.5) as regenerant, SBB and WBB were regenerated with nearly 100% recovery of adsorption capacity over ten consecutive adsorption-desorption cycles. Straw-based biochar and wood-based biochar are efficient sorbents for removal of water-soluble ionic liquids from aqueous solutions.

1. Introduction

Ionic liquids (ILs) are a series of synthetic room-temperature molten salts consisting of large asymmetrical organic cations (e.g., alkylimidazolium) paired with inorganic/organic anions (e.g., BF_4^-, PF_6^-) (Bubalo et al., 2014). Due to their unique physicochemical characteristics such as low-volatility, non-flammability, high ionic conductivity and thermal stability (Martínez-Palou and Luque, 2014), ILs have been widely used as alternatives to classical organic solvents in the field of green synthesis, catalysis and separation processes (Plechkova and Seddon, 2008). The growing application of ILs in chemical industries has increased their opportunity for release into the environment (Amde et al., 2015; Thi et al., 2010). IL contaminants in effluents have shown low biodegradability and high toxicity or inhibitory effects towards green algae and activated sewage sludge organisms or inhibitory effects on their growth and physiological activities (Liu et al., 2015; Markiewicz et al., 2013). Therefore, appropriate treatment technologies should be developed to dispose of ILs-containing wastewaters.

Artificial methods for destruction of ILs in wastewaters include biodegradation, ultrasonic degradation, electrolytic degradation, UV photodegradation and fenton/fenton-like reactions (Amde et al., 2015). Adsorption is the primary nondestructive technique applied in the treatment of ILs-contained waters due to the recovery potential of ILs. Activated carbon (AC) adsorption is a potential separation method for removing ILs from effluents (Lemus et al., 2012; Palomar et al., 2009). However, the adsorption efficiencies for ILs, even by high-surface-area ACs, are poor (Qi et al., 2013), which is presumably due to their inherent surface hydrophobicity. ILs are usually classified as hydrophilic or hydrophobic in terms of the length of the alkyl chain of IL cations as well as the type of IL anions (Huddleston et al., 2001). Most ILs containing short-alkyl-chain cations ($C_n < 4$), are hydrophilic, which means they have low octanol-water partition coefficients (K_{ow}, 10^{-3}–10^{-1}) and low water solubility (Hassan et al., 2014; Lee and Lin, 2014). Some ILs are composed of long-alkyl-chain cations ($C_n > 4$) and strongly coordinating anions (e.g.,1-hexyl-3-methylimidazolium bis[(trifluoromethyl)sulfonyl]imide or $[C_6mim][NTf_2]$) making them hydrophobic in character. However, their K_{ow} still remain low (< 2) (Ropel et al., 2005), which are smaller by 2–4 orders of magnitude than many persistent organic pollutants (POPs). Thus, the adsorption of ILs on ACs is significantly less than that of many POPs.

* Corresponding author at: State Key Laboratory of Pollution Control and Resource Reuse, College of Environmental Science and Engineering, Tongji University, Shanghai 200092, China.
E-mail addresses: ypqiu@tongji.edu.cn, ypqiu@g.ucla.edu (Y. Qiu).

http://dx.doi.org/10.1016/j.ecoenv.2016.04.017
0147-6513/

AC modification by physical or chemical treatments can improve AC pore structure and/or increase the carbon surface groups, thereby enhancing its adsorption affinity to ILs, but may be costly. Biochar, a kind of eco-friendly biomass-derived carbon, has been receiving considerable attention for its ability to remove contaminants, sequester carbon and improve soil fertility (Ahmad et al., 2014; Singh et al., 2010). Biochar is a porous solid material generated from the direct pyrolysis of a sustainable natural biomass (e.g. crop residues, wood, manure and other waste feed stocks) in an oxygen-limited environment (Lehmann and Joesph, 2009). It is regarded as a greener and less expensive adsorbent to replace AC for removal of contaminants from wastewaters (Li et al., 2014).

Typical biochar has less carbonized structure, less surface area but more surface polar functional groups than AC (Azargohar and Dalai, 2006). Qi et al. (2013) prepared a cellulose-derived carbonaceous material (CCM), with surface area only 2% of that of AC. However, the uptake of 1-butyl-3-methylimidazolium chloride on CCM was almost equal to that of AC. They further found that the chemical activation with KOH to CCM had positive effect on hydrophilic ILs sorption, which they attributed to the increase of polar oxygenated surface groups on CCM (Qi et al., 2014). It seems that biochar with more hydrophilic structure would be more suitable for adsorption of polar or ionic chemicals compared with commercial ACs.

Recently, the high sorption of ionic organic compounds on biochar, such as ionizable veterinary antibiotics (Zheng et al., 2013) and water-soluble dyes (Qiu et al., 2009), has been widely reported. For example, wood-based biochar showed the unbelievable adsorption coefficient (K_d) of sulfamethazine ($K_{ow}=1.86$) as high as 10^6 L/kg, which was due to the coupling of coulombic attraction, π^+-π electron-donor-acceptor (EDA) interaction and H-bonding between hydrophilic adsorbate and biochar surface (Teixidó et al., 2011). Analogously, biochar might also be considered a high efficiency absorbent for removal of ionizable ILs from wastewaters.

In the present study, straw- and wood-based biochars with different surface properties and pore size distribution were prepared to test their ability to absorb hydrophilic or hydrophobic imidazolium-type ionic liquids (ITILs). The adsorption effects caused by solution pH and the background cations/anions with different charges were also investigated. Additionally, batch adsorption-desorption tests were conducted to compare the removal efficiency of ITILs by biochars from wastewaters. The object of this work is to clarify the influence of structures and characteristics of both adsorbate and adsorbent on the adsorption of ITILs by biochars, to assess the adsorption effectiveness of ITILs on different biochars, and to discuss the potential application of biochar as a new efficient adsorbent for ITILs removal.

2. Materials and methods

2.1. Materials

Five types of ITILs (purity $>98\%$) with different alkyl-chain cations and different anions were purchased from Shanghai Chengjie Chemical Co. Ltd and listed in Table 1S. All of them were used without additional purification. The straw-derived biochar was prepared according to Qiu et al. (2008). In brief, the ashes from the burned rice straws (*Oryza sativa* L.) were collected and treated by 0.5 mol l^{-1} HCl–HF solution (1:1) three times for removal of Si. After washed with distilled water, the straw-derived biochars named SBB were attained until the effluent pH increased to above 7.0. The wood-derived biochars named WBB were obtained by slow-pyrolyzing from peeled wood chips (*Ziziphus jujuba* L.) at 700 °C for 6 h under oxygen-limited conditions. SBB and WBB were crushed and passed through a nylon sieve with 0.154 mm openings. Wood-based commercial powdered activated carbon (PAC) was donated by Calgon Carbon Co. Limited (Suzhou, China).

The specific surface area (S_{BET}) of biochars and PAC was evaluated from the N_2 adsorption (77 K) isotherms by applying the Brunauer–Emmett–Teller (BET) method using Micromeritics ASAP-2020M (Norcross, GA, USA). Pore volume distributions were analyzed through the application of Density Functional Theory (DFT). Scanning electron microscopy/energy dispersive X-ray spectroscopy (SEM/EDX) was used to investigate the morphological and chemical composition of carbon particles. The percentage of carbon and oxygen in biochars and PAC was determined by EDX analysis. The surface oxygen functional groups of carbons were determined using Boehm's titration method (Qiu et al., 2008). Fourier transform infrared spectroscopy (FT-IR) was recorded by a Nicolet 5700 spectrophotometer (Thermo Electron Scientific Instruments Corp., USA). The biochar samples were scanned in 32 scans over the range from 4000 to 500 cm^{-1} with a resolution of 4 cm^{-1}. Each spectrum of biochar before and after adsorption was collected to discuss the potential adsorption mechanism for ITILs.

2.2. Batch sorption experiments

Batch adsorption experiments were carried out in 22 mL glass tubes with ~0.08 g biochar or AC samples and 20 mL ITILs solutions (0.5–3 mmol L^{-1}). Various concentrations of ITILs were prepared with 0.01 M (NaCl) ionic strength solution. All tubes were capped and rotated end-over-end at 40 rpm to mix the contents at 25 °C for 36 h. No ITILs volatilization or degradation occurred during the sorption process, as verified by HPLC analysis. The preliminary tests showed that the sorption of ITILs on SBB, WBB and AC reached equilibrium within 24 h (Fig. 1S). After attainment of equilibrium, the solution was filtered using 0.45 μm-pore-size membrane syringe filters and then analyzed for ITILs concentration by HPLC. All the adsorption experiments were performed in duplicate, and the

Table 1
Selected physicochemical properties of the powder activated carbon, straw-based biochar and wood-based biochar.

	C (%)	O (%)	O/C	S_{BET} ($m^2 g^{-1}$)	D (nm)	V_{total} ($cm^3 g^{-1}$)	V_{micro} ($cm^3 g^{-1}$)	V_{micro}/V_{total}	Surface acidity (mmol g^{-1})	Surface basicity (mmol g^{-1})
Powder activated carbon	90.34 ± 0.02	8.24 ± 0.02	0.091	1268.2	2.43	1.164	0.258	0.222	ND*	ND*
Straw-based biochar	86.45 ± 0.05	12.37 ± 0.03	0.143	733.1	4.88	0.894	0.099	0.111	0.89 ± 0.06	0.71 ± 0.04
Wood-based biochar	93.45 ± 0.04	6.55 ± 0.01	0.070	464.8	2.42	0.281	0.174	0.619	0.27 ± 0.02	0.45 ± 0.01

* ND = Not determined.

data were presented as the mean values with the maximum relative standard deviation (RSD) lower than ±6.0%.

2.3. Adsorption-desorption tests for [C_2mim][BF_4]

2.3.1. Comparison of adsorption and desorption isotherms

Adsorption of [C_2mim][BF_4] by SBB and WBB was performed using the above-mentioned batch equilibration method. The working solutions contained [C_2mim][BF_4] (1.0 mmol L^{-1} to 4.5 mmol L^{-1}) and Na_3PO_4 (0.01 mol L^{-1}). After reaching equilibrium, all tubes were centrifuged at 2000 rpm for 10 min. 15 mL of the supernatant was replaced with 15 mL 0.01 mol L^{-1} Na_3PO_4 solution to observe desorption.

2.3.2. Continuous adsorption-desorption cycle tests

0.01 mol L^{-1} Na_3PO_4 was used as background solution to enhance the adsorption of [C_2mim][BF_4]. After achieving batch adsorption equilibrium, the supernatant of [C_2mim][BF_4] was removed as completely as possible by centrifugation. Subsequently, 20 mL HCl solution (pH ~0.5) was added in tubes and shaken for 24 h at 25 °C to desorb [C_2mim][BF_4] from SBB or WBB. After that, the solution was centrifuged and then removed for the next adsorption–desorption equilibrium experiment, and the [C_2mim][BF_4] concentrations in the supernatant and the acidic regenerant were determined. The tests were repeated ten times to test the potential application of SBB and WBB for continuous adsorption-desorption of [C_2mim][BF_4]. The desorption efficiency of [C_2mim][BF_4] in each cycle was calculated as follows: Desorption (%)=(the number of moles of [C_2mim][BF_4] adsorbed onto biochars)/(the number of moles of [C_2mim][BF_4] desorbed from biochars) × 100%.

2.4. ITILs analysis

The amount of sorbed ITILs on carbons was determined by direct analysis of the filtrate using Agilent 1200 Series HPLC System with a reverse-phase column (Waters C_{18}, 5 μm, 4.6 × 250 mm; Waters, Milford, MA, USA). ITILs concentrations were identified via an UV detector at a wavelength of 218 nm, with a flow rate of 1 mL/min and sample size of 10 μL. The mobile phase was mixed with acetonitrile and 5 mM pH 3.0 phosphate buffer (30/70%, v/v). Prior to the analysis, all solvents were filtered through 0.45 μm-pore-size membrane syringe filters. All filters used in this did not adsorb the ITILs.

2.5. Data fitting

All sorption and desorption isotherm data are fitted by the Freundlich equation,.

$$q_e = K_f \cdot C_e^n \quad (1)$$

where q_e (mmol g^{-1}) and C_e (mmol L^{-1}) are the amount of ITILs adsorbed and the equilibrium concentration, respectively. K_f [(mmol g^{-1})/(mmol L^{-1})^n] is a constant representing the sorption capacity. n is the parameter describing the nonlinearity of isotherms, respectively. Apparent distribution coefficients K_d (L g^{-1}) were calculated by q_e/C_e to compare different ITILs adsorption at identical equilibrium concentration (e.g. C_e=1.0 mmol l^{-1}).

3. Results and discussion

3.1. Structural properties of carbons and their gerneral adsorption of ITILs

Under the same pyrolysis conditions, straw-based biochar (SBB) and wood-based biochar (WBB) showed different microstructures and different surface characteristics, which were probably related to their structures of original biomass precursors (feedstocks). Rice straw consists of hollow-tubular culms while *Ziziphus jujuba* L. is a high density hard wood. Accordingly, SBB exhibited loose porous texture, morphologically similar to the PAC used in this study (Fig. 2S a and b). In contrast, WBB showed the highly compact and microporous packing structure (Fig. 2S c).

SEM/EDX analysis revealed the high C elemental contents and the presence of oxygen (Table 1). The O/C ratio of SBB (0.143) was twice as high as that of WBB (0.070), suggesting the existence of more surface oxygen-containing groups on SBB surface. It was consistent with the Boehm's titration result where the surface acidity of SBB (0.089) was 3.30 times higher than that of WBB (0.027). The N_2 adsorption-desorption isotherm for SBB and PAC features significant hysteresis loops at high relative pressure (P/P_0) range of 0.5–1.0 (Fig. 1a), indicative of their mesoporous nature. However, WBB exhibited a type I isotherm with nearly a flat isotherm. Additionally, the adsorption/desorption hysteresis loop of WBB is scarcely visible, implying micropores would be dominantly presented in WBB structure. The micropore volume (V_{micro}) of WBB (0.174 cm^3 g^{-1}) is 1.76 times higher than that of SBB (0.099 cm^3 g^{-1}) (Table 1) though its surface area (S_{BET}) and total pore volume (V_{total}) are lower than that of SBB. PAC has a higher V_{micro} value than WBB. However, its V_{micro}/V_{total} ratio is 2.79 times less than that of WBB. The results were in good agreement with the pore size distribution of carbons (Fig. 1b), in which WBB exhibited a narrow pore distribution with a main peak value of

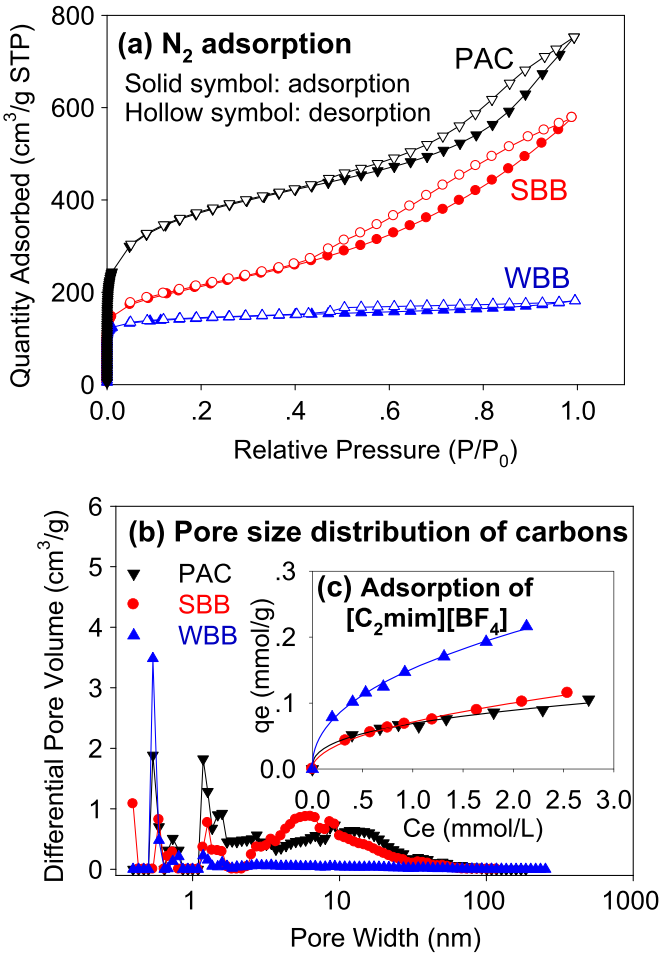

Fig. 1. (a) N_2 adsorption-desorption isotherms of PAC, SBB and WBB, (b) pore size distribution curves of PAC, SBB and WBB, (c) General adsorption of [C_2mim][BF_4] on PAC, SBB and WBB at pH 7.10 at 25 °C.

around 0.54 nm, while both SBB and PAC displayed a wide mesopore distribution between 2 and 50 nm.

Although commercial PAC has a high surface area and large pore volume produced by a well-controlled activation process, it does not exhibit perfect adsorption ability for ITILs. By comparison, both SBB and WBB samples, fabricated without any activation process, have a significantly lower surface area. However, SBB showed a similar adsorption capacity of $[C_2mim][BF_4]$ to PAC (Fig. 1c). It seems that the surface area is not a key factor controlling ITILs adsorption. The higher molar O/C ratio of SBB is associated with higher hydrophilicity of SBB and may help to facilitate the formation of polar interactions between SBB surface and hydrophilic ITILs. Compared to the effect of surface hydrophilicity, supermicroporosity may play a more important role in the overall adsorption of ITILs. WBB exhibits the highest adsorption of $[C_2mim][BF_4]$ because it has the highest proportion of micropores (61.9% of total pore volume) among three carbons. These results indicate biochars (SBB and WBB) have greater adsorption potential than AC and might be considered as a suitable AC substitute to remove ITILs from aqueous solutions.

3.2. Adsorption of ITILs on SBB

The adsorption of a homologous series of 1-alkyl-3-methylimidazolium tetrafluoroborate cations with different lengths of alkyl chain (C_2, C_4 and C_5) and different fluorine-containing anions on SBB is illustrated in Fig. 2a and b. All isotherms fit well to the Freundlich equation and all the values of n are less than 1, suggesting a concentration-dependent type of adsorption.

With a constant anion of tetrafluoroborate, a considerable increase in K_d value is observed as the length of the straight alkyl chains of ITILs increased. When the n-alkyl chain length on the cation varied from ethyl to pentyl, the K_d of ITILs increases 3.63 times (Table 2S). Further analysis reveals that the K_d of $[C_nmim][BF_4]$ on SBB is linearly proportional to the number of carbon atoms (n) in alkyl chains of $[C_nmim]^+$ cations with the correlation coefficients (R^2) larger than 0.999 (Fig. 2c). The sorption experiment showed similar result with natural soils, where the log K_d of alkyl imidazolium cations correlated reasonably well with n (R^2 from 0.94 to 0.98). Lemus et al. (2012) also found that the adsorption of homologous ITILs on commercial activated carbons varied directly with the rise of molar volume of ITIL cations, relating the total number of carbon atoms in their substituents. These results suggested that an increase of hydrophobic nature of ITILs with a larger alkyl chain would enhance the hydrophobic interactions between cations and adsorbents, thereby favoring the adsorption of ITILs.

Fig. 2(b) shows that the adsorption of ITILs strongly depends on the counter anion of ITILs. The K_d of ITILs on SBB are ranked from $[BF_4]^- < [PF_6]^- < [NTf_2]^-$, which is in accordance with the sequence of the hydrophobicity of anions. $[C_2mim][BF_4]$ is the most hydrophilic for its complete dissociation in water at the concentration examined in the study. Therefore, the adsorption of $[C_2mim][BF_4]$ is actually the adsorption of $[C_2mim]^+$ cation. In contrast, the anions of $[PF_6]^-$ and $[NTf_2]^-$ are expected to drive dissociation of ion pairs with $[C_2mim]^+$ cation. The ITILs bearing the anion $[NTf_2]^-$ exist predominantly in the associative state, suggestive of its highest hydrophobicity among three anions (Yee et al., 2013). According to Lee and Lin (2014), the logarithms of 1-octanol-water partition coefficient (log K_{ow}) of $[C_2mim][BF_4]$, $[C_2mim][PF_6]$ and $[C_2mim][NTf_2]$ are −2.66, −2.36 and −1.18, respectively. It is interesting to observe a positive linear relationship between the K_d of ITILs with different anions on SBB and their log K_{ow} (Fig. 2(c)). The low R^2 value (0.833) presumably indicates that the anion-induced hydrophobic interactions are not the dominant interaction between ITILs and SBB surface.

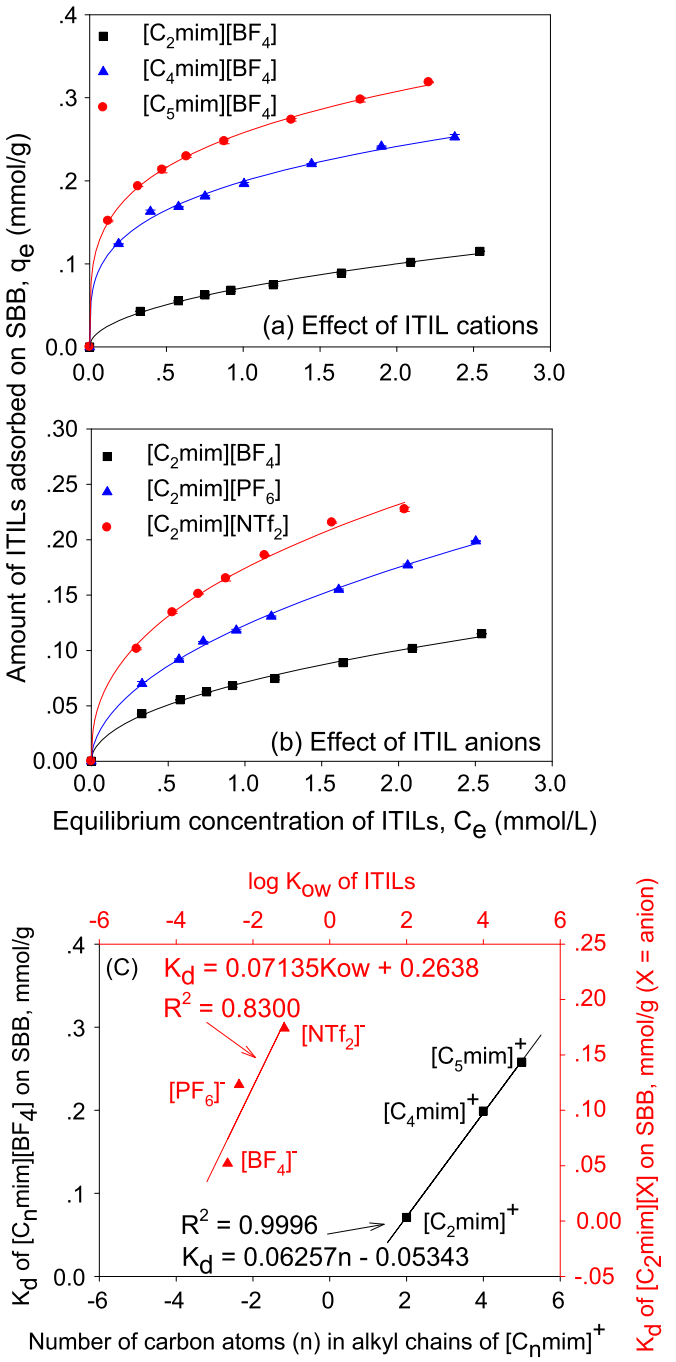

Fig. 2. Adsorption of $[C_nmim][BF_4]$ by SBB at pH 7.10 at 25 °C: effect of (a) of alkyl chain length of ITIL cations, $C_n = C_2$, C_4 and C_5; effect of (b) ITIL anions types, $[BF_4]^-$, $[PF_6]^-$ and $[NTf_2]^-$. (c) the relationship between K_d of $[C_nmim][BF_4]$ on SBB and the number of carbon atoms (n) in alkyl chains of $[C_nmim]^+$ cations (black line); the relationship between K_d of $[C_nmim][BF_4]$ on SBB and the K_d of ITILs with different anions (red line). (For interpretation of the references to color in this figure legend, the reader is referred to the web version of this article.)

3.3. Adsorption of ITILs on WBB

Due to existence of more fine pore structures, WBB shows a much higher K_d value for ITILs than SBB (Table 2S). The ratio of V_{micro}/V_{total} of WBB (61.9%) is 5.8 times greater than that of SBB (11.1%), which results in the predominance of volume filling adsorption on WBB. Micropore filling theory considers that multiple walls of micropores easily form an overlapping adsorption force thereby causing the enhanced volume uptake of ITILs solutes (Mosher et al., 2013). A similar micropore-filling effect was found

in the previous study of high-temperature-prepared (micropore-dominated) biochars which showed that they adsorb more sulfonamides than low-temperature prepared (macropore-dominated) biochars (Xie et al., 2014). However, micropore-dominated WBB has no adsorption advantage for ITILs containing imidazolium cations with long alkyl chains, compared with $[C_4mim][BF_4]$ and $[C_5mim][BF_4]$. In general, the increase of alkyl-chain length not only enhances ITILs hydrophobicity but also enlarges ITILs molecule size. Fig. 1(b) shows that WBB contains mostly primary micropores (pore width <0.8 nm), which are inaccessible to these large molecules or cations. Previous studies demonstrated that adsorption to micropore structure may occur as the pore size is 1.7 times the molecule's second widest dimension (Pelekani and Snoeyink, 2000). The cation size (length × width × thickness) of $[C_4mim]^+$ has been reported as 1.19 nm × 0.62 nm × 0.4 nm (Hassan et al., 2014). Consequently, $[C_4mim]^+$ cations are difficult to enter the primary micropore in WBB because the $[C_4mim]^+$ cation's second widest dimension is 1.05 nm, which is larger than the primary micropore width of 0.8 nm. A similar pore blockage will be observed for the larger$[C_5mim]^+$ cations. It is no wonder that $[C_5mim][BF_4]$ displays the same adsorption to $[C_4mim][BF_4]$.

ITILs with the hydrophilic anion ($[BF_4]^-$) and hydrophobic anions ($[PF_6]^-$ and $[NTf_2]^-$) show similar adsorption capacity on WBB (Fig. 3(b)), which is different from the adsorption on SBB. Since $[C_2mim][BF_4]$ is fully dissociated in dilute solutions (Boruń et al., 2015), the adsorption of $[C_2mim][BF_4]$ on WBB is dependent upon the adsorption of $[C_2mim]^+$ cations. By comparison, hydrophobic anions easily form ion-pair association by conjugating with methylimidazolium cation. These ion-pair structures are larger than either respective cations or anions. Moreover, both $[PF_6]^-$ and $[NTf_2]^-$ anions contain six fluorine atoms, which tend to combine with water molecule clusters via hydrogen bonding (Tran et al., 2003). The large ion-pair volume of $[C_2mim][PF_6]$ and $[C_2mim][NTf_2]$ prevents them from entering the primary micropore regions on WBB. It seems that the steric hindrance effect (adsorption reduction) will largely counteract the influence of ITILs hydrophobicity (adsorption enhancement). Therefore, WBB is unsuitable for adsorption of ITILs with large molecule size.

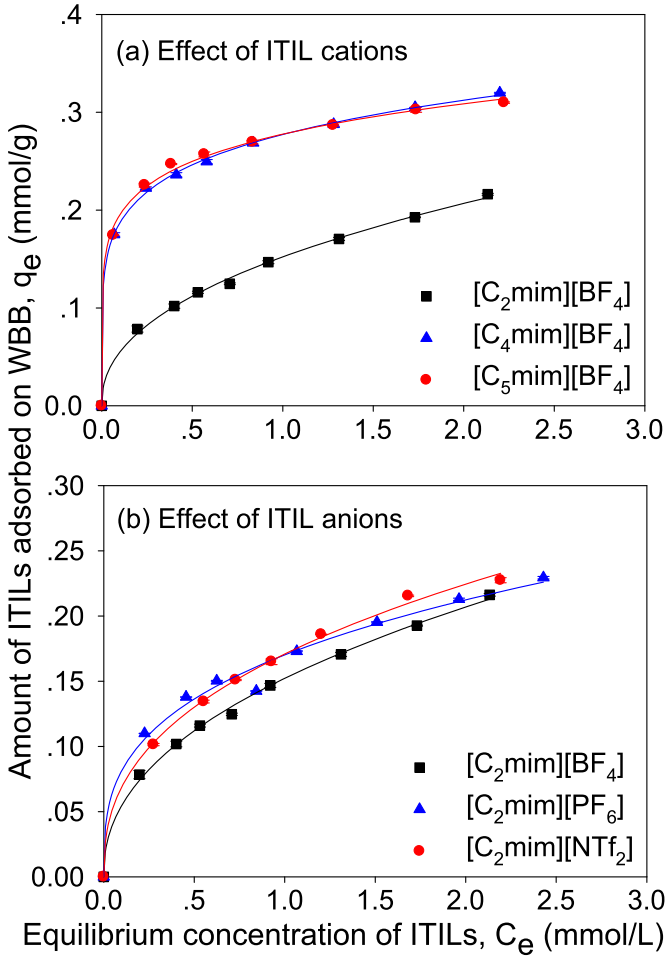

Fig. 3. Adsorption of $[C_nmim][BF_4]$ by WBB at pH 7.10 at 25 °C: effect of (a) of alkyl chain length of ITIL cations, $C_n=C_2$, C_4 and C_5; effect of (b) ITIL anions types, $[BF_4]^-$, $[PF_6]^-$ and $[NTf_2]^-$.

3.4. Using FITR for exploring adsorption mechanisms of ITILs on SBB and WBB

Due to the special structure of with different alkyl chain length and anion species, ITILs show multiple adsorption mechanisms with solid adsorbents (e.g. soils), such as ion exchange, ion pairing, hydrophobic bonding, π-π bonds, and Van der Waals forces (Mrozik et al., 2008). Farooq et al. (2012) speculated that the adsorption of $[C_4mim][Cl]$ on activated carbons was controlled by electrostatic interactions rather than dispersive ones (e.g. hydrophobic bonding, π-π bonds). This hypothesis is based on the comparison of the adsorption capacities of ITILs at acidic and alkaline pHs, but without direct spectroscopic evidence. In this work, the spectroscopic mechanism of ITILs adsorption is explored using FTIR spectra. Both FTIR spectra for SBB and WBB before and after ITILs adsorption are depicted in Fig. 3S. The original SBB shows two characteristic absorption peaks of 3416.1 and 1620.6 cm^{-1}, which are assigned to the stretching vibrations of O–H and the unsymmetric stretching vibrations of C=O, respectively (Özçimen and Ersoy-Meriçboyu, 2010). Similar bands are found on the original WBB at 3447.8 and 1638.1 cm^{-1}. After adsorption of ITILs on SBB, different hypsochromical shifts of two characteristic peaks for three kinds of ITILs are observed. The shift of the corresponding O–H and C=O peaks ranged from 1.4 to 8.3 cm^{-1} and 5.7–12.7 cm^{-1}, respectively. It is evidence of the participation of –C–OH and –C=O groups on the surface of SBB in the electrostatic binding of $[C_2mim]^+$ cations. In general, hydrophilic ITILs, $[C_2mim][BF_4]$, exhibiit higher shifts than hydrophobic ITILs ($[C_2mim][PF_6]$ and $[C_2mim][NTf_2]$), which is attributed to the greater $[C_2mim]^+$ cations in aqueous solution due to the complete dissociation of $[C_2mim][BF_4]$. In contrast, PF_6^-or NTf_2^-anions tend to form partial ion-pairs (association) with ITIL cations (Katsuta et al., 2008). Therefore, less $[C_2mim]^+$ in water will cause weaker electrostatic interactions between ITILs and biochar surfaces. Similar FTIR analysis has been used by Xu et al. (2011) to understand the adsorption mechanism of methyl violet on biochars derived from crop residues. They also found the blue shift on the oxygen-containing groups after adsorption of the dye. This means that the adsorption mechanism of methyl violet on biochars is electrostatic attraction, which is a specific interaction between the cationic dye and the groups of –COO– and phenolic –OH. In another case, visible changes in intensity and shift of peaks of the phenolic –OH stretching and the C=O stretching in the carbon aromatic ring were observed in the FTIR spectra of biochar after adsorbing malachite green (Leng et al., 2015). However, WBB shows negligible blue shifts of two characteristic stretching vibration peaks (0.2–0.8 cm^{-1} for –OH and 0.2–0.3 cm^{-1} for –C=O) after adsorption of three kinds of ITILs (Fig. 3S -b). The surface functional groups on WBB are only approximately 30% of that on SBB (Table 1). Therefore, the electrostatic interactions may not play a primary role in the adsorption of ITILs on WBB due to the absence of available adsorption sites.

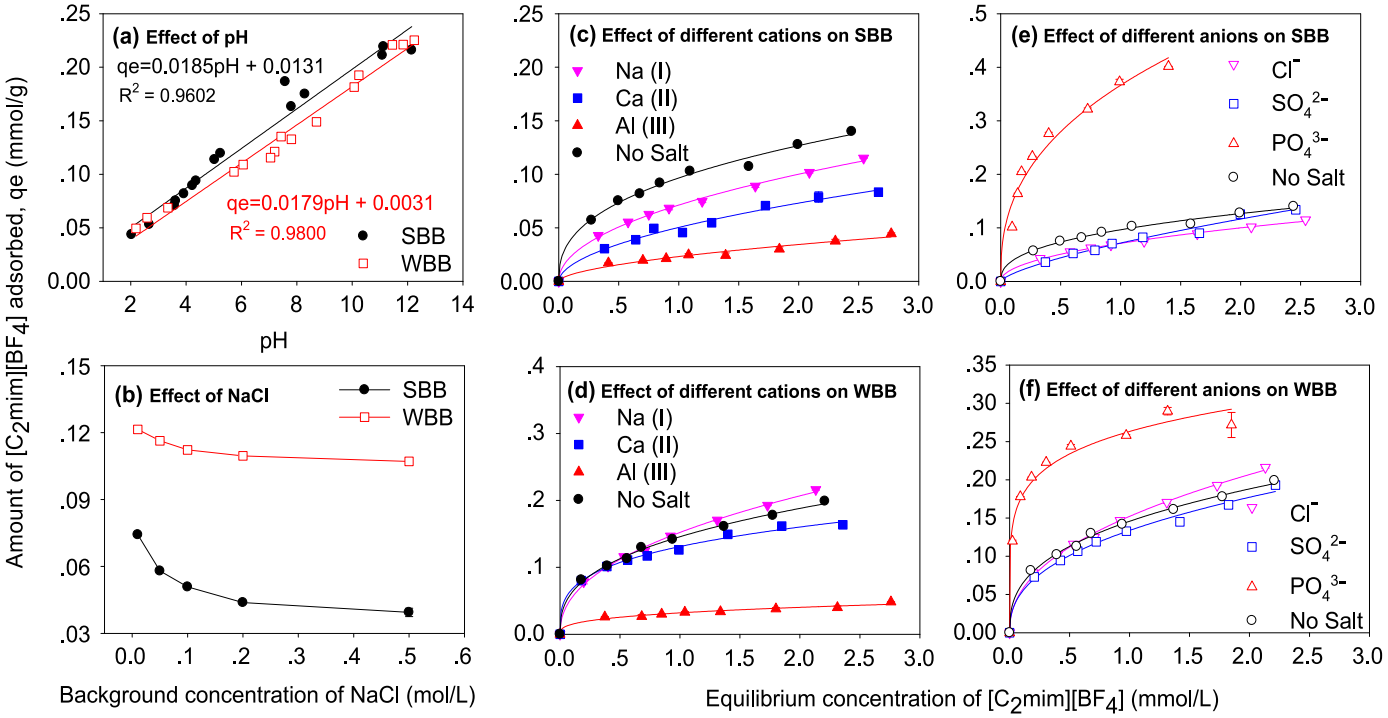

Fig. 4. The amounts of $[C_2mim][BF_4]$ adsorption on SBB and WBB determined using an initial $[C_2mim][BF_4]$ concentration of 1 mmol l^{-1} at 25 °C (a) as affected by pH ranging from 2.0–12.0 at ionic strength of 0.01 mol l^{-1} NaCl solution; (b) as a function of NaCl concentration ranging from 0.01 to 0.5 mol l^{-1}. Adsorption of $[C_2mim][BF_4]$ onto (c) SBB and (d) WBB as affected by 0.01 mol l^{-1} Na (I), Ca (II) and Al (III); Adsorption of $[C_2mim][BF_4]$ onto (e) SBB and (f) WBB as affected by 0.01 mol l^{-1} Cl^-, SO_4^{2-}, and PO_4^{3-}(equilibrium pH 7.10, 25 °C).

3.5. *Effect of pH and background cations/anions of different valences*

Environmental factors, such as solution pH and the coexisting electrolytes in water, strongly affect ionic organics adsorption. Solution pH significantly influences the surface chemistry of biochars as well as the sorbate species in solution (Qiu et al., 2008). Due to the acidity/basicity of surface functional groups, the surface of biochar has a net charge resulting from protonation/deprotonation of these dissociable functional groups (Yang et al., 2004). At different pH values, the carbon surface will have a net positive or negative electric charge, thereby influencing ITILs adsorption on biochars. The adsorption of hydrophilic ITILs, $[C_2mim][BF_4]$, was investigated as a function of pH over the range of 2.0 to 12.0. Fig. 4a shows that the adsorption on both biochar samples increased monotonically with increasing pH. At low pH, the surface of biochars has a net positive charge resulting in attractive forces that are overcome by electrostatic repulsion. Conversely, the negatively charged surface at high pH will promote the adsorption of $[C_2mim]^+$ cations due to the enhanced electrostatic attraction. The equilibrium uptakes of SBB and WBB at pH 12.0 are approximately 5.1 and 4.2 times greater than at pH 2.0, respectively. It suggests that SBB and WBB can be used for adsorbing hydrophilic ITILs from water at alkaline pH and then recovering the adsorbed ITILs using acidic regenerate solutions. In the pH range studied, the amount of $[C_2mim][BF_4]$ adsorbed on SBB and WBB linearly increases with increasing solution pH (R^2 of 0.96 and 0.98, respectively). The slope of line of SBB (0.0185) is similar to that of WBB (0.0179) and the correlations are quite similar (Fig. 4a), which indicates that the pH-dependent uptake of $[C_2mim][BF_4]$ on biochars is independent of biochar type and their structure characteristics.

The effect of the background ionic strength (univalent NaCl solution) on the adsorption of $[C_2mim][BF_4]$ by SBB and WBB is shown in Fig. 4b. The adsorbed amount of $[C_2mim][BF_4]$ on biochars declines moderately with the growing NaCl concentration from 0.01 to 0.5 mol L^{-1}. It is the result of the screening effect of a growing partial neutralization of negative charges on biochars by Na^+ cations. Another explanation is that more Na^+ cations cause more intensive competition for adsorption sites (e.g. deprotonated carboxyl groups) with $[C_2mim]^+$ cations. The decline of $[C_2mim][BF_4]$ uptake onto SBB (46.9%) is higher than that onto WBB (11.8%), which is due to the presence of more oxygen-containing groups on the surface of SBB.

Background salts consisting of a series of 0.01 mol l^{-1} monovalent, divalent and trivalent cations (or anions) were comprehensively tested for their ability to influence the amount of $[C_2mim][BF_4]$ adsorbed on SBB and WBB. Fig. 4c–d and Table 3S exhibit greater inhibition of divalent Ca (II) and trivalent Al (III) on adsorption of $[C_2mim][BF_4]$ than monovalent Na (I) due to their greater abilities of compressing the electrical double layer of biochars. The stronger effect of Al (III) is due partly to the existence of some insoluble aluminum hydroxide at the experimental pH, which may block the micropores and cover the surface of biochars. The influence mechanism of background anions on $[C_2mim][BF_4]$ adsorption is more complex than background cations. In this work, anions, whether monovalent Cl^- or divalent SO_4^{2-}, have no significant impact on $[C_2mim][BF_4]$ adsorption (Fig. 4e and f). However, trivalent PO_4^{3-} dramatically enhances the adsorption of $[C_2mim][BF_4]$ by K_d % of 279.4% and 80.6% on SBB and WBB, respectively. It is because PO_4^{3-}, as a kind of salting-out salt, can attract the solvent water molecules and disrupt the interaction between the water and ITILs. Hence, it would result in a decrease of relative solubility of ITILs in water and therefore largely improve their adsorption onto biochars. The observation is in good agreement with Neves et al. (2014) who showed that the presence of the salting-out salt in water can greatly enhance the adsorption of hydrophilic $[C_4mim][Cl]$ and $[C_4mim][CH_3SO_3]$ on activated carbons. The salting-out phenomenon of polyvalent anions is also supported by predictions of the change of log K_{ow} of hydrophilic ITILs in the presence and in the absence of salt using the quantum-chemical COSMO-RS method. As the salt concentration of polyvalent anions

increases in aqueous solution, hydrophobic interactions will therefore increase because a higher log K_{ow} value of ITILs is obtained (Neves et al., 2014).

3.6. Potential application of biochars for removal of ITILs from aqueous solutions

Using 0.01 mol L^{-1} Na_3PO_4 background solution as a desorbing agent, SBB shows negligible irreversible adsorption of [C_2mim][BF_4] (Fig. 5a, Table 4S), which is presumably due to the existence of strong binding between [C_2mim] cations and SBB surface. However, the adsorption and desorption isotherms of WBB completely overlap (Fig. 5b) because the adsorption of [C_2mim][BF_4] on WBB is a reversible physical adsorption process. These observations are in accord with our prior FTIR analysis (Fig. 3S).

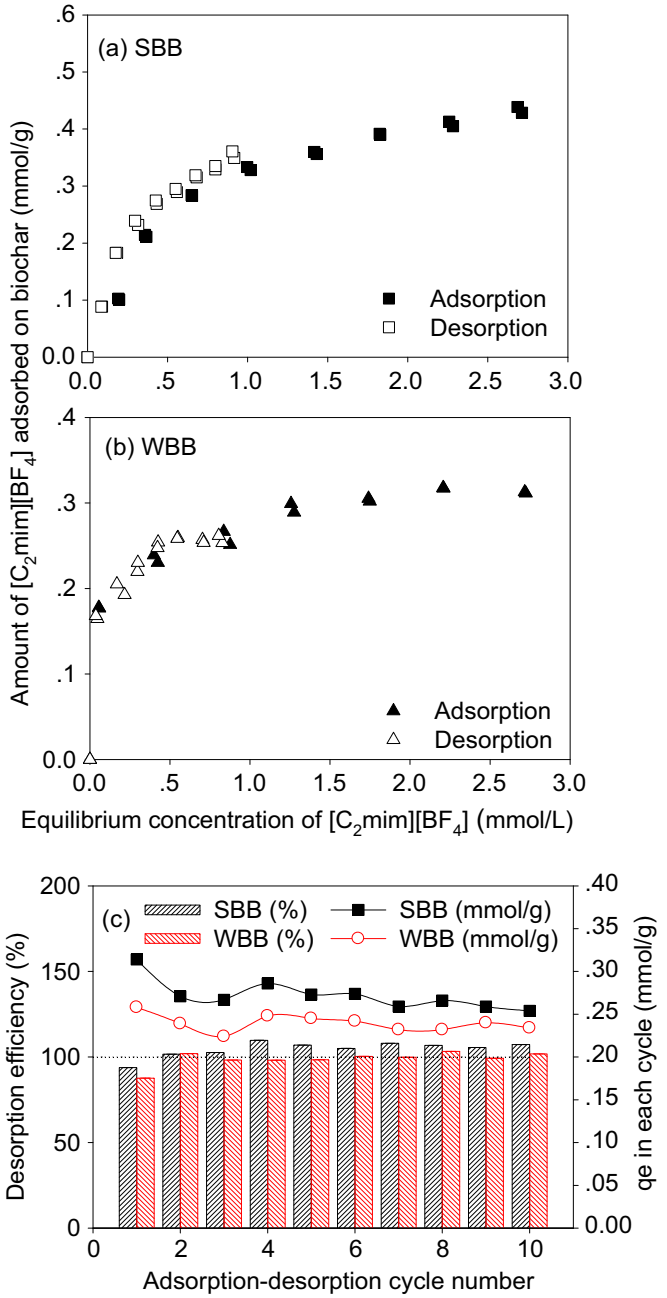

Fig. 5. Adsorption and desorption of [C_2mim][BF_4] on (a) SBB and (b) WBB in 0.01 mol/l Na_3PO_4 solution; (c) Continuous desorption efficiency of [C_2mim][BF_4] by SBB and WBB during the adsorption-desorption cycle tests (adsorption background solution: 0.01 mol/l Na_3PO_4 with unadjusted pH; the initial concentration of [C_2mim][BF_4]: 2 mmol/l; solution volume: 20 mL; dosage of biochars, 2.5 g/L. Desorption conditions: 25 °C for 24 h; desorbing agent, 20 mL aqueous solution (pH=0.5, adjusted by HCl; dosage of biochars, 2.5 g/L).

To explore potential application of biochars for ITIL removal from wastewater, continuous (Ten times) adsorption-desorption experiments were conducted to test the adsorption stability and regeneration performance. 0.5 mol L^{-1} HCl solutions were used as a desorbing agent to improve the regenerability of biochars. For the first cycle, desorption efficiencies of SBB and WBB were 93.8% and 87.7%, respectively (Fig. 5c), which is probably related to the residual impurities in pores. After the first adsorption-desorption procedure, the desorption efficiencies (DE%) for both biochars stabilize at nearly 100% throughout the remaining nine cycles and their adsorption capacities (q_m) remain about 0.26 and 0.23 mmol g^{-1} for SBB and WBB, respectively. The performance indices, including DE%, q_m, and cycle times, are superior to the reported data on carbon microspheres derived from hydrothermal carbonization of cellulose (Qi et al., 2013). Our study indicated that SBB and WBB are potentially efficient adsorbents for recovery of water-soluble ionic liquids from wastewater. Further studies of fixed-bed or column adsorption will be performed in the future to better understand the application of biochars for ITILs removal.

4. Conclusions

In this work, we developed two biochars derived from straw and wood (SBB and WBB, respectively) to improve the adsorption effectiveness for removal of ITILs from wastewaters. SBB had abundant oxygen-containing functional groups, while WBB displayed a high percentage of micropores. Both of them exhibited greater ITILs adsorption effectiveness than high-surface-area activated carbon. FTIR spectra revealed that electrostatic interactions were the dominant driving force on SBB. In contrast, micropore-filling effect promoted ITILs adsorption on WBB. Adsorption of ITILs (e.g. [C_2mim][BF_4]) on SBB and WBB is pH-dependent and can be significantly enhanced by trivalent PO_4^{3-} anions due to salting-out effect. The adsorbed [C_2mim][BF_4] are easily desorbed with HCl solution (pH 0.5) and the adsorbents could be reused up to ten adsorption-desorption cycles without losing high adsorption efficiency. Our results showed that both SBB and WBB are efficient sorbents for removal of water-soluble ionic liquids from wastewaters.

Acknowledgement

This research was supported by the National Natural Science Foundation of China (21377093 and 21177113) and the China Scholarship Council (File no. 201406265021).

Appendix A. Supporting information

Supplementary data associated with this article can be found in the online version at http://dx.doi.org/10.1016/j.ecoenv.2016.04.017.

References

Özçimen, D., Ersoy-Meriçboyu, A., 2010. Characterization of biochar and bio-oil samples obtained from carbonization of various biomass materials. Renew. Energy 35, 1319–1324.

Ahmad, M., Rajapaksha, A.U., Lim, J.E., Zhang, M., Bolan, N., Mohan, D., Vithanage, M., Lee, S.S., Okm, Y.S., 2014. Biochar as a sorbent for contaminant management in soil and water: a review. Chemosphere 99, 19–33.

Amde, M., Liu, J.F., Pang, L., 2015. Environmental application, fate, effects, and concerns of ionic liquids: a review. Environ. Sci. Technol. 49, 12611–12627.
Azargohar, R., Dalai, A.K., 2006. Biochar as a precursor of activated carbon. Appl. Biochem. Biotechnol. 129–132, 762–773.
Boruń, A., Fernandez, C., Bald, A., 2015. Conductance studies of aqueous ionic liquids solutions [emim][BF_4] and [bmim][BF_4] at temperatures from (283.15 to 318.15) K. Int. J. Electrochem. Sci. 10, 2120–2129.
Bubalo, M.C., Radošević, K., Redovniković, I.R., Halambek, J., Srček, V.G., 2014. A brief overview of the potential environmental hazards of ionic liquids. Ecotoxicol. Environ. Saf. 99, 1–12.
Farooq, A., Reinert, L., Leveque, J.M., Papaiconomou, N., Irfan, N., Duclaux, L., 2012. Adsorption of ionic liquids onto activated carbons: effect of pH and temperature. Microporous Mesoporous Mater. 158, 55–63.
Hassan, S., Duclaux, L., Lévêque, J.-M., Reinert, L., Farooq, A., Yasin, T., 2014. Effect of cation type, alkyl chain length, adsorbate size on adsorption kinetics and isotherms of bromide ionic liquids from aqueous solutions onto microporous fabric and granulated activated carbons. J. Environ. Manag. 144, 108–117.
Huddleston, J.G., Visser, A.E., Reichert, W.M., Willauer, H.D., Broker, G.A., Rogers, R. D., 2001. Characterization and comparison of hydrophilic and hydrophobic room temperature ionic liquids incorporating the imidazolium cation. Green Chem. 3, 156–164.
Katsuta, S., Yamaguchi, N., Ogawa, R., Kudo, Y., Takeda, Y., 2008. Distribution of 1-alkyl-3-methylimidazolium ions and their ion pairs between dichloromethane and water. Anal. Sci. 24, 1261–1267.
Lee, B.-S., Lin, S.-T., 2014. A priori prediction of the octanol–water partition coefficient (K_{ow}) of ionic liquids. Fluid Phase Equilib. 363, 233–238.
Lehmann, J., Joesph, S., 2009. Biochar for Environmental Management: Science and Technology. Earthscan, London.
Lemus, J., Palomar, J., Heras, F., Gilarranz, M.A., Rodriguez, J.J., 2012. Developing criteria for the recovery of ionic liquids from aqueous phase. Sep. Purif. Technol. 97, 11–19.
Leng, L.J., Yuan, X.Z., Zeng, G.M., Shao, J.G., Chen, X.H., Wu, Z.B., Wang, H., Peng, X., 2015. Surface characterization of rice husk bio-char produced by liquefaction and application for cationic dye (Malachite green) adsorption. Fuel 155, 77–85.
Li, L., Qiu, Y.P., Huang, J.X., Li, F.L., Sheng, G.D., 2014. Mechanisms and factors influencing adsorption of microcystin-LR on biochars. Water Air Soil Pollut. 225, 2220.
Liu, H.J., Zhang, X.Q., Chen, C.D., Du, S.T., Dong, Y., 2015. Effects of imidazolium chloride ionic liquids and their toxicity to Scenedesmus obliquus. Ecotoxicol. Environ. Safe 122, 83–90.
Markiewicz, M., Piszora, M., Caicedo, N., Jungnickel, C., Stolte, S., 2013. Toxicity of ionic liquid cations and anions towards activated sewage sludge organisms from different sources – consequences for biodegradation testing and wastewater treatment plant operation. Water Res. 47, 2921–2928.
Martínez-Palou, R., Luque, R., 2014. Applications of ionic liquids in the removal of contaminants from refinery feedstocks: an industrial perspective. Energ. Environ. Sci. 7, 2414–2447.
Mosher, K., He, J.J., Liu, Y.Y., Rupp, E., Wilcox, J., 2013. Molecular simulation of methane adsorption in micro- and mesoporous carbons with applications to coal and gas shale systems. Int. J. Coal Geol. 109–110, 36–44.
Mrozik, W., Jungnickel, C., Skup, M., Urbaszek, P., Stepnowski, P., 2008. Determination of the adsorption mechanism of imidazolium-type ionic liquids onto kaolinite: implications for their fate and transport in the soil environment. Environ. Chem. 5, 299–306.
Neves, C.M.S.S., Lemus, J., Freire, M.G., Palomar, J., Coutinho, J.A.P., 2014. Enhancing the adsorption of ionic liquids onto activated carbon by the addition of inorganic salts. Chem. Eng. J. 252, 305–310.
Palomar, J., Lemus, J., Gilarranz, M.A., Rodríguez, J.J., 2009. Adsorption of ionic liquids from aqueous effluents by activated carbon. Carbon 47, 1846–1856.
Pelekani, C., Snoeyink, V.L., 2000. Competitive adsorption between atrazine and methylene blue on activated carbon: The importance of pore size distribution. Carbon 38, 1423–1436.
Plechkova, N.V., Seddon, K.R., 2008. Applications of ionic liquids in the chemical industry. Chem. Soc. Rev. 37, 123–150.
Qi, X.H., Li, L.Y., Tan, T.F., Chen, W.T., Smith Jr., R.L., 2013. Adsorption of 1-butyl-3-methylimidazolium chloride ionic liquid by functional carbon microspheres from hydrothermal carbonization of cellulose. Environ. Sci. Technol. 47, 2792–2798.
Qi, X.H., Li, L.Y., Wang, Y., Liu, N., Smith Jr., R.L., 2014. Removal of hydrophilic ionic liquids from aqueous solutions by adsorption onto high surface area oxygenated carbonaceous material. Chem. Eng. J. 256, 407–414.
Qiu, Y.P., Cheng, H.Y., Xu, C., Sheng, G.D., 2008. Surface characteristics of crop-residue-derived black carbon and lead (II) adsorption. Water Res. 42, 567–574.
Qiu, Y.P., Zheng, Z.Z., Zhou, Z.L., Sheng, G.D., 2009. Effectiveness and mechanisms of dye adsorption on a straw-based biochar. Bioresour. Technol. 100, 5348–5351.
Ropel, L., Belvèze, L.S., Aki, S.N.V.K., Stadtherr, M.A., Brennecke, J.F., 2005. Octanol–water partition coefficients of imidazolium-based ionic liquids. Green Chem. 7, 83–90.
Singh, B., Singh, B.P., Cowie, A.L., 2010. Characterisation and evaluation of biochars for their application as a soil amendment. Soil Res. 48, 516–525.
Teixidó, M., Pignatello, T.T., Beltrán, J.L., Granados, M., Peccia, J., 2011. Speciation of the ionizable antibiotic sulfamethazine on black carbon. Environ. Sci. Technol. 45, 10020–10027.
Thi, P.T.P., Cho, C.W., Yun, Y.S., 2010. Environmental fate and toxicity of ionic liquids: a review. Water Res. 44, 352–372.
Tran, C.D., De Paoli Lacerda, S.H., Oliveira, D., 2003. Absorption of water by room-temperature ionic liquids: effect of anions on concentration and state of water. Appl. Spectrosc. 57, 152–157.
Xie, M., Chen, W., Xu, Z., Zheng, S., Zhu, D., 2014. Adsorption of sulfonamides to demineralized pine wood biochars prepared under different thermochemical conditions. Environ. Pollut. 186, 187–194.
Xu, R.K., Xiao, S.C., Yuan, J.H., Zhao, A.Z., 2011. Adsorption of methyl violet from aqueous solutions by the biochars derived from crop residues. Bioresour. Technol. 102, 10293–10298.
Yang, Y., Chun, Y., Sheng, G., Huang, M., 2004. pH-dependence of pesticide adsorption by wheat-residue-derived black carbon. Langmuir 20, 6736–6741.
Yee, P., Shah, J.K., Maginn, E.J., 2013. State of hydrophobic and hydrophilic ionic liquids in aqueous solutions: are the ions fully dissociated? J. Phys. Chem. B 117, 12556–12566.
Zheng, H., Wang, Z., Zhao, J., Herbert, S., Xing, B., 2013. Sorption of antibiotic sulfamethoxazole varies with biochars produced at different temperatures. Environ. Pollut. 181, 60–67.